

## Enabling DMG Wi-Fi Sensing in Data Transmission Intervals by Exploiting Beam Training Codebook

Attiah, Kareem; Wang, Pu; Mansour, Hassan; Koike-Akino, Toshiaki; Boufounos, Petros T.

TR2025-026 March 08, 2025

### Abstract

This paper addresses the integration of millimeter-wave (mmWave) Wi-Fi communication and sensing during data transmission intervals (DTIs). We leverage prior knowledge from codebook beam training conducted during preceding beacon transmission intervals (BTIs) and association beamforming training (A-BFT) intervals to design a transceiver array response that meets both requirements on downlink communication SNR and targeted sensing area. By formulating it as a first-order array response optimization with constraints on power, codebook, communication SNR, and limited RF chains, this paper introduces a two-stage solution. First, we introduce a two-way communication-sensing matching pursuit to determine a set of codewords that prioritize the communication SNR constraint. Then, using the selected codewords, we employ an alternating minimization over an auxiliary phase term and beamforming weights to further minimize an array-response distance loss. Numerical results validate the effectiveness of the proposed DMG beamforming design over baseline methods.

*IEEE International Conference on Acoustics, Speech, and Signal Processing (ICASSP) 2025*



# Enabling DMG Wi-Fi Sensing in Data Transmission Intervals by Exploiting Beam Training Codebook

Kareem M. Attiah<sup>1,2</sup>, Pu (Perry) Wang<sup>1</sup>, Hassan Mansour<sup>1</sup>, Toshiaki Koike-Akino<sup>1</sup>, Petros Boufounos<sup>1</sup>

<sup>1</sup>Mitsubishi Electric Research Laboratories (MERL), Cambridge, MA 02139, USA

<sup>2</sup>University of Toronto, Toronto, Canada

**Abstract**—This paper addresses the integration of millimeter-wave (mmWave) Wi-Fi communication and sensing during data transmission intervals (DTIs). We leverage prior knowledge from codebook beam training conducted during preceding beacon transmission intervals (BTIs) and association beamforming training (A-BFT) intervals to design a transceiver array response that meets both requirements on downlink communication SNR and targeted sensing area. By formulating it as a first-order array response optimization with constraints on power, codebook, communication SNR, and limited RF chains, this paper introduces a two-stage solution. First, we introduce a two-way communication-sensing matching pursuit to determine a set of codewords that prioritize the communication SNR constraint. Then, using the selected codewords, we employ an alternating minimization over an auxiliary phase term and beamforming weights to further minimize an array-response distance loss. Numerical results validate the effectiveness of the proposed DMG beamforming design over baseline methods.

**Index Terms**—Wi-Fi sensing, directional Multi-Gigabit (DMG), beam training, WLAN Sensing, 802.11bf, beamforming, ISAC.

## I. INTRODUCTION

In the on-going developments of the IEEE 802.11bf WLAN Sensing Standards, Wi-Fi sensing is categorized into *sub-7-GHz Wi-Fi sensing* and *directional multi-gigabit (DMG) Wi-Fi sensing* operating at frequencies above 45 GHz with certain privacy and security measures [1]. At a typical range of 10 meters, Wi-Fi signals at 60 GHz experience an additional 22-dB attenuation compared to the propagation loss at 5 GHz [2]–[5]. As a result, directional beamforming is crucial to compensate for this significant path loss.

DMG Wi-Fi sensing can be integrated at different phases or time intervals of the DMG Wi-Fi communication. As shown in Step 1 of Fig. 1 (a), the AP initiates downlink beam training during the beacon transmission interval (BTI), where each communication user calculates the received beam SNRs for the transmitted directional beampatterns. In the subsequent association beamforming training (A-BFT) interval (see Step 2 of Fig. 1 (a)), users may train their uplink directional beampatterns by transmitting directional beams at the user end and optionally providing feedback on the received SNRs from the BTI to the AP. Once the best downlink-uplink beampattern pair is established, high-throughput data transmission takes place during the data transmission interval (DTI) in Step 3 of Fig. 1 (a).

Corresponding Wi-Fi sensing technologies have been developed in these DMG time intervals. For **BTI sensing**, a passive sensing receiver can be placed within the environment [6]–[17] (see Fig. 1(b) for a monostatic configuration) to capture reflections of the directional beams transmitted by the AP. Specifically, [6] proposed a generalized likelihood ratio test (GLRT) to detect a single object by leveraging the

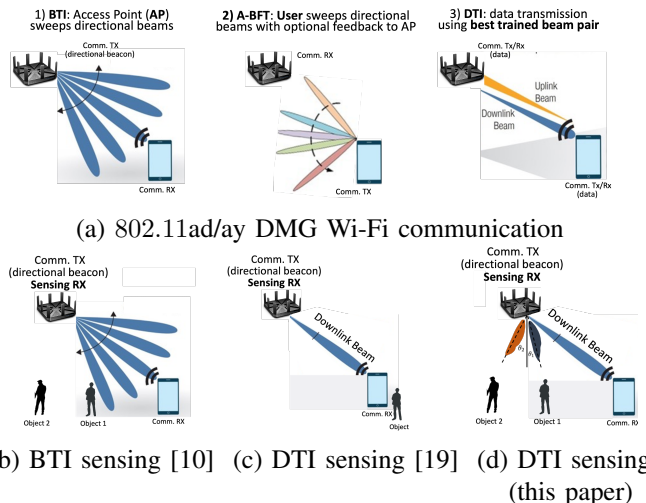


Fig. 1: (a) Directional beam training and directional data transmission defined in 802.11ad/ay; (b) BTI sensing that reuses directional beacon frames from AP for sensing [7]–[10]; (c) DTI sensing of objects within downlink beam [19]–[21]; (d) DTI sensing with beamforming design (this paper).

structure (preamble, header, data fields) of the control PHY (CPHY) frame used during the BTI. This approach was extended in [7] to handle multiple objects, and further refined in [8] using a subspace method in the delay-Doppler domain. [9] and [10] further addressed the coupling between frame-to-frame TX-RX antenna gain, caused by the misalignment between probing sector beampatterns and the object steering vector, and the frame-based slow-time Doppler steering vector. **A-BFT sensing** can similarly be enabled using approaches developed for BTI sensing [18]. For **DTI sensing**, [19] and [20] pioneered the reuse of single-carrier physical layer (SCPHY) data frames for automotive radar applications but limited the targets within the main beam of identified downlink-uplink beampatterns, e.g., the case that the communication user is also the object; see Fig. 1(c). Following [19], [21] proposed a modified data frame sequence for robust performance particularly in detecting moving objects.

Assuming an additional sensing receiver (RX) is deployed at the AP in a monostatic configuration (see Fig. 1(d)), this paper proposes an integrated DTI communication and sensing scheme with adaptive beamforming to overcome the limitation that objects must be within the main beam of the trained downlink beampattern [19], [20]. Specifically, we adopt a codebook beamforming approach that aims to match a desired array response over a given angle interval for object sensing, while adhering to power constraints, downlink communication SNR requirements, and limited RF chains. More importantly, our scheme does not require prior knowledge of the

K. M. Attiah is a PhD student at University of Toronto. This work was done during his internship at MERL.

communication channel between the AP and users by leveraging downlink beam training during the BTI and the optional feedback mechanism during A-BFT. This is achieved by introducing a two-stage optimization. First, we introduce a two-way communication-sensing matching pursuit to select a set of codewords to be used by the AP to prioritize the communication link SNR and account for sensing performance. Then, given these selected codewords, we employ an alternating minimization between an auxiliary phase term and the beamforming weights to match a desired array response.

## II. SIGNAL MODEL AND PROBLEM FORMULATION

As shown in Fig. 2, AP sends sector sweep (SSW) frames  $s_g(t)$  sequentially using directional beampatterns or codebook  $\mathbf{f}_k \in \mathbb{C}^{N_T}$  during *BTI beam training* to identify the best downlink beam to be used in DTI. Specifically, the SSW frame is given as

$$s_g(t) = \sqrt{E_s} \sum_{l=0}^{L-1} s_l g_{\text{TX}}(t - lT_s), \quad (1)$$

where  $E_s$  is the symbol energy,  $s_l$  is the modulated symbol after  $\pi/2$ -BPSK modulation with alphabet of  $\{\pm 1, \pm i\}$ ,  $g_{\text{TX}}(t)$  is the baseband pulse (e.g., a pair of TX and RX filter for error vector magnitude measurement as a root-raised cosine (RRC) filter with a roll-off factor of 0.25),  $T_s = 1/B$  is the symbol interval with  $B$  denoting the channel bandwidth, and  $L$  is the number of symbols.

Modulated with the carrier frequency  $f_c$  and weighted by the beamforming codebook  $\mathbf{f}_k$ , the  $k$ -th SSW frame is given as

$$x_k(t) = \mathbf{f}_k s_g(t - kT_p) e^{j2\pi f_c t}, \quad (2)$$

where  $T_p$  is the pulse repetition interval (PRI). Assuming a geometric channel model with  $N_s$  scatterers between the AP and a user, the communication channel matrix can be expressed as

$$\mathbf{H}_{\text{comm}} = \sum_{i=1}^{N_s} \alpha_i \mathbf{a}_{R,\text{comm}}(\theta_i) \mathbf{a}_T^H(\phi_i), \quad (3)$$

where  $\alpha_i$  represents the amplitude over the  $i$ -th path with  $\theta_i$  and  $\phi_i$  denoting associated angular angle-of-departure (AoD) and angle-of-arrival (AoA), and  $\mathbf{a}_{R,\text{comm}}(\theta_i) \in \mathbb{C}^{N_R}$  and  $\mathbf{a}_T(\phi_i) \in \mathbb{C}^{N_T}$  are, respectively, angular channel steering vectors.

On the user side, a pseudo-omni-directional receiving beampattern  $\mathbf{f}_{\text{comm}} \in \mathbb{C}^{N_R}$  is employed for all  $K$  probing codewords. After applying carrier demodulation and a matched filter with respect to the baseband pulse  $g_{\text{RX}}(t) = g_{\text{TX}}(t)$ , the quality of each probing codeword can be calculated as

$$\begin{aligned} \eta_k &= \mathbf{f}_{\text{comm}}^H \mathbf{H}_{\text{comm}} \mathbf{f}_k \sqrt{E_s} \sum_{l=0}^{L-1} |s_l|^2 \\ &\quad \times \left| \int_t \left| \int_z g_{\text{RX}}(z) g_{\text{TX}}(t - kT_p - lT_s - z) dz \right|^2 dt \right. \\ &\stackrel{(a)}{=} \mathbf{f}_{\text{comm}}^H \mathbf{H}_{\text{comm}} \mathbf{f}_k (\sqrt{E_s} L E_g) \end{aligned} \quad (4)$$

where (a) holds due to the fact that the integral over  $z$  yields the baseband pulse matched filter output, i.e., a raised cosine pulse shifted at the delay  $kT_p + lT_s$  and that the subsequent integral over  $t$  computes its energy  $E_g$  which remains invariant to the delay  $kT_p + lT_s$ . Given the noise variance  $\sigma^2$  and assuming without loss of generality that  $\sigma^2 = \sqrt{E_s} L E_g$ , the downlink beam SNR for each codeword is obtained as

$$\gamma_k = \frac{\eta_k}{\sigma^2} = \mathbf{f}_{\text{comm}}^H \mathbf{H}_{\text{comm}} \mathbf{f}_k. \quad (5)$$

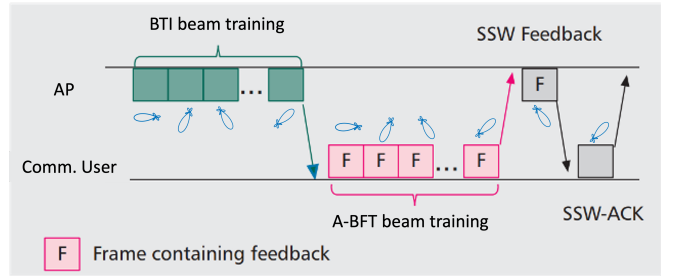


Fig. 2: DMG codebook-based beam training protocols during BTI and A-BFT.

Then, during *A-BFT beam training* of Fig. 2, the user transmits similar SSW frames to the AP using its uplink beamforming codebook so that the AP can compute the corresponding uplink beam SNRs to identify the best uplink beam to be used by the user. Each of these uplink SSW frames may contain feedback fields, allowing the user to share downlink beam SNRs  $\gamma_k$  back to the AP so that the AP can identify the best downlink beam to send a follow-up SSW Feedback frame to the user. The SSW Feedback frame informs the user of the best uplink beam for the uplink communication. Finally, the user uses the best uplink beam to send an SSW-ACK frame to the AP to confirm the completion of downlink and uplink beam training.

To enable integrated DTI communication and sensing, we are interested in designing a joint transceiver beamformer  $\mathbf{f}_T$  and  $\mathbf{f}_R$  such that the resulting downlink communication SNR

$$|\mathbf{f}_{\text{comm}}^H \mathbf{H}_{\text{comm}} \mathbf{f}_T|^2 = |\mathbf{h}_c^H \mathbf{f}_T|^2 \geq \tau \quad (6)$$

where  $\mathbf{h}_c \triangleq \mathbf{H}_{\text{comm}}^H \mathbf{f}_{\text{comm}}$ , is above a threshold to guarantee the communication link quality. Following the standard specifications of existing DMG Wi-Fi devices, we assume that the AP is equipped with a hybrid architecture with  $L$  RF chains. Therefore, the transmit beamformer is formed as

$$\mathbf{f}_T = \sum_{k=1}^K w_k \mathbf{f}_k = \mathbf{F} \mathbf{w}, \quad \|\mathbf{w}\|_0 \leq L \quad (7)$$

where  $\|\mathbf{w}\|_0$  denotes the  $\ell_0$ -norm and  $\mathbf{F} \in \mathbb{C}^{N_T \times K}$  is a given codebook of size  $K$ . We emphasize that the DTI transmit beamforming vector  $\mathbf{f}_T$  is based on exactly the same codebook  $\mathbf{F}$  used during the BTI and constructed as a linear combination of at most  $L$  codewords. This allows for the calculation of downlink communication SNR for a chosen DTI transmit beamforming vector  $\mathbf{f}_T$  using only the BTI feedback  $\{\gamma_k\}_{k=1}^K$ , thereby eliminating the need to know or estimate the communication channel  $\mathbf{H}_{\text{comm}}$ , i.e.,

$$|\mathbf{f}_{\text{comm}}^H \mathbf{H}_{\text{comm}} \mathbf{f}_T|^2 = \left| \sum_k w_k \gamma_k \right|^2 = |\boldsymbol{\gamma}^T \mathbf{w}|^2, \quad (8)$$

where  $\boldsymbol{\gamma} = [\gamma_1, \dots, \gamma_K]^T$  is the calculated BTI communication SNRs at the user that were fed back to AP during A-BFT. We further impose a power constraint on both transmit and (sensing) receive beamformers as

$$\mathbf{f}_T^H \mathbf{f}_T = P_T, \quad \mathbf{f}_R^H \mathbf{f}_R = P_R. \quad (9)$$

We aim to optimize the beamformers to match some desired array response for sensing while satisfying the communication SNR and power constraints. Let  $\mathbf{A}_T = [\mathbf{a}_T(\theta_1), \dots, \mathbf{a}_T(\theta_{N_g})] \in \mathbb{C}^{N_T \times N_g}$  and  $\mathbf{A}_R = [\mathbf{a}_R(\theta_1), \dots, \mathbf{a}_R(\theta_{N_g})] \in \mathbb{C}^{N_R \times N_g}$  denote matrices of array responses at pre-determined grid values over AoD

and AoA angles. Then, we design the beamformers to minimize  $\|\mathbf{D}_T \boldsymbol{\mu}_T - \mathbf{A}_T^H \mathbf{f}_T\|$  for the transmit side and  $\|\mathbf{D}_R \boldsymbol{\mu}_R - \mathbf{A}_R^H \mathbf{f}_R\|$  for the receive side, where  $\boldsymbol{\mu}_T \in \mathbb{R}^{N_g}$  and  $\boldsymbol{\mu}_R \in \mathbb{R}^{N_g}$  are nominal desired responses, which can be chosen depending on some prior belief on potential objects. The auxiliary phase matrices  $\mathbf{D}_T$  and  $\mathbf{D}_R$  are diagonal matrices with  $[\mathbf{D}]_{nn} = e^{j\phi_n}$  for unknown phase angles  $\phi_n$ . These matrices are introduced to allow the beamformed response to match a phase-rotated version of the nominal response, since all phase-rotated versions will exhibit the same performance. Accounting for the constraints on downlink communication SNR (6), codebook (7) and power (9), the optimization is expressed as

$$\underset{\mathbf{D}_T, \mathbf{f}_T, \mathbf{w}}{\text{minimize}} \quad \|\mathbf{D}_T \boldsymbol{\mu}_T - \mathbf{A}_T^H \mathbf{f}_T\| \quad (10a)$$

$$\text{s. t.} \quad \mathbf{f}_T = \mathbf{F} \mathbf{w}, \quad (10b)$$

$$|\mathbf{h}_c^H \mathbf{f}_T|^2 \geq q, \quad (10c)$$

$$\mathbf{f}_T^H \mathbf{f}_T = P_T, \quad (10d)$$

$$\|\mathbf{w}\|_0 \leq L. \quad (10e)$$

for the transmitter side. Further, for the receiver side, we have

$$\underset{\mathbf{D}_R, \mathbf{f}_R}{\text{minimize}} \quad \|\mathbf{D}_R \boldsymbol{\mu}_R - \mathbf{A}_R^H \mathbf{f}_R\|, \quad \text{s. t.} \quad \mathbf{f}_R^H \mathbf{f}_R = P_R. \quad (11)$$

### III. PROPOSED SOLUTION

We focus on designing the transmit beamformer and defer the discussion of the receive beamformer until the end of this section. Directly identifying the optimal codewords requires a combinatorial search through  $\binom{K}{L}$  configurations. For example, in typical 802.11ay settings with  $K = 32$  and  $L = 4$ , this results in 35960 possibilities. Even with a pre-selected codebook, the problem remains nonconvex due to the auxiliary phase matrix  $\mathbf{D}_T$  and the nonconvex constraints (10c)-(10d). In this section, we propose a computationally efficient solution with two stages. In Stage I, we introduce a two-way communication-sensing matching pursuit approach to select codewords, effectively defining the support of  $\mathbf{w}$ . In Stage II, we address the resulting subproblem with an alternating minimization between  $\mathbf{D}_T$  and beamforming weight  $\mathbf{w}$  over the selected support.

#### A. Two-way Matching Pursuit for Codeword Selection

We start by reformulating problem (10) into an equivalent form

$$\underset{\mathbf{D}_T, \mathbf{w}}{\text{minimize}} \quad \|\boldsymbol{\mu}_T - \mathbf{D}_T^H \mathbf{A}_T^H \mathbf{F} \mathbf{w}\| \quad (12a)$$

$$\text{subject to} \quad |\mathbf{h}_c^H \mathbf{F} \mathbf{w}|^2 \geq q, \quad (12b)$$

$$\mathbf{w}^H \mathbf{F}^H \mathbf{F} \mathbf{w} = P_T, \quad (12c)$$

$$\|\mathbf{w}\|_0 \leq L. \quad (12d)$$

where the equivalence follows from the fact that  $\mathbf{D}_T$  is a unitary matrix. Problem (12) can be interpreted as a sparse recovery problem, where the objective is to approximate the desired array response  $\boldsymbol{\mu}_T$  using  $L$  atoms (i.e., column vectors) selected from a dictionary given by  $\mathbf{D}_T^H \mathbf{A}_T^H \mathbf{F}$ . Unlike conventional sparse recovery problems, however, problem (12) allows for flexibility in designing the dictionary by optimizing over the auxiliary diagonal phase matrix  $\mathbf{D}_T$ . Additionally, the beamforming solution  $\mathbf{w}$  must satisfy constraints for the downlink communication SNR (12b) and power (12c), in addition to approximating the target array response vector  $\boldsymbol{\mu}_T$ .

To this end, we propose a two-way matching pursuit algorithm that chooses the codewords in the direction of either the communication or sensing. Like the classical OMP, the proposed algorithm selects the codewords from  $\mathbf{F}$  iteratively by maximizing their inner product with a residual vector at each step. However, the key difference lies

in how the residual vector is computed. Let  $\mathbf{F}_\ell \in \mathbb{C}^{N_T \times \ell}$  denote the matrix of selected codewords at the  $\ell$ -th step. At each step, the algorithm first solves the following optimization problem

$$\underset{\mathbf{w}}{\text{maximize}} \quad |\mathbf{h}_c^H \mathbf{F}_\ell \mathbf{w}|^2, \quad \text{s. t.} \quad \mathbf{w}^H \mathbf{F}_\ell^H \mathbf{F}_\ell \mathbf{w} = P_T, \quad (13)$$

whose closed-form solution is given by  $\tilde{\mathbf{w}}_\ell^* = \sqrt{P_T} \frac{\mathbf{F}_\ell^\dagger \mathbf{h}_c}{\|\mathbf{F}_\ell \mathbf{F}_\ell^\dagger \mathbf{h}_c\|}$  with  $\mathbf{F}^\dagger \triangleq (\mathbf{F}^H \mathbf{F})^{-1} \mathbf{F}^H$  denoting the pseudo inverse of  $\mathbf{F}$ . The optimal value of (13) serves as a feasibility check of whether a given selection of codewords  $\mathbf{F}_\ell$  satisfies the communication SNR constraint (12b). If it exceeds  $q$ , i.e.,

$$|\mathbf{h}_c^H \mathbf{F}_\ell \tilde{\mathbf{w}}_\ell^*|^2 = P_T \|\mathbf{F}_\ell \mathbf{F}_\ell^\dagger \mathbf{h}_c\|^2 \geq q, \quad (14)$$

there exists a set of nonzero weights that would linearly combine the column vectors in  $\mathbf{F}_\ell$  to yield a beamforming vector satisfying the communication constraint (12b). Conversely, if  $P_T \|\mathbf{F}_\ell \mathbf{F}_\ell^\dagger \mathbf{h}_c\|^2 < q$ , constraint (12b) is violated for all beamformers that are written as a linear combination of the columns in  $\mathbf{F}_\ell$ .

The proposed codeword selection strategy chooses subsequent codewords based on whether the feasibility condition (14) is satisfied. If condition (14) fails at step  $\ell$ , the next chosen codeword should be close to the direction of communication vector  $\mathbf{h}_c$  to further enhance the downlink communication link. This is achieved by performing one more iteration of the classical OMP to approximate  $\mathbf{h}_c$  using codewords drawn from a dictionary  $\mathbf{F}$ , given that  $\ell < L$  columns  $\mathbf{F}_\ell$  have been previously selected. This leads to the computation of a residual term  $\mathbf{r}_\ell = \mathbf{h}_c - \mathbf{F}_\ell \hat{\mathbf{w}}_\ell$  between the communication vector  $\mathbf{h}_c$  and already identified codewords  $\mathbf{F}_\ell$ , where the weight for the  $L$  codewords is given by

$$\hat{\mathbf{w}}_\ell = \arg \min_{\mathbf{w}} \|\mathbf{h}_c - \mathbf{F}_\ell \mathbf{w}\| = \mathbf{F}_\ell^\dagger \mathbf{h}_c. \quad (15)$$

and the selection of the next codeword that maximizes the inner product between  $\mathbf{r}_\ell$  and the remaining codewords  $\mathbf{f} \in \mathbf{F}/\mathbf{F}_\ell$ ,

$$\mathbf{f}_{\ell+1} = \arg \max_{\mathbf{f} \in \mathbf{F}/\mathbf{F}_\ell} |\mathbf{r}_\ell^H \mathbf{f}|. \quad (16)$$

On the other hand, if condition (14) is satisfied at step  $\ell$ , the chosen codewords already meet the communication SNR constraint, and the next codeword should be selected to optimize the sensing performance. This is done by performing one more iteration of the OMP to find a sparse approximation of  $\boldsymbol{\mu}$  using an adaptive dictionary  $\mathbf{D}_T^H \mathbf{A}_T^H \mathbf{F}$ , given that  $\mathbf{D}_T^H \mathbf{A}_T^H \mathbf{F}_\ell$  have previously been selected. In this case, the iteration involves solving the following minimization

$$\{\hat{\mathbf{D}}_\ell, \hat{\mathbf{w}}_\ell\} = \arg \min_{\mathbf{D}, \mathbf{w}} \|\boldsymbol{\mu} - \mathbf{D}_T^H \mathbf{A}_T^H \mathbf{F}_\ell \mathbf{w}\|, \quad (17)$$

then computing the residual  $\mathbf{r}_\ell = \boldsymbol{\mu} - \hat{\mathbf{D}}_\ell^H \mathbf{A}_T^H \mathbf{F}_\ell \hat{\mathbf{w}}_\ell$ , and finally selecting the next codeword according to

$$\begin{aligned} \mathbf{f}_{\ell+1} &= \arg \max_{\mathbf{f} \in \mathbf{F}/\mathbf{F}_\ell} \max_{\mathbf{D}_T} |\mathbf{r}_\ell^H \mathbf{D}_T^H \mathbf{A}_T^H \mathbf{f}| \\ &= \arg \max_{\mathbf{f} \in \mathbf{F}/\mathbf{F}_\ell} \sum_{n=1}^{N_g} |\mathbf{r}_\ell[n]| \cdot |[\mathbf{A}_T^H \mathbf{f}]_n|. \end{aligned} \quad (18)$$

As the proposed method can either select the codewords to enhance the downlink communication link (15)-(16), or to improve the sensing (17)-(18), we refer to it as two-way matching pursuit. Finally, the new codeword is appended to the existing set of selected codewords as

$$\mathbf{F}_{\ell+1} = [\mathbf{F}_\ell \quad \mathbf{f}_{\ell+1}]. \quad (19)$$

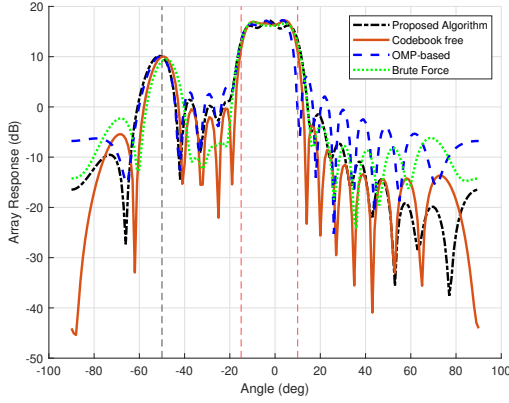


Fig. 3: Transmit beampatterns of all considered methods. The communication user at  $-50^\circ$  has a downlink SNR constraint of 10 dB and the sensing interval of interest spans  $[-15^\circ, 10^\circ]$ .

### B. Optimization over $\mathbf{D}_T$ and $\mathbf{w}$ for Selected Codewords

Given the selected codeword  $\mathbf{F}_L$  from the two-way matching pursuit method, we may simplify problem (12) as follows

$$\underset{\mathbf{D}_T, \mathbf{w}}{\text{minimize}} \quad \|\boldsymbol{\mu}_T - \mathbf{D}_T^H \mathbf{A}_T^H \mathbf{F}_L \mathbf{w}\|^2 \quad (20a)$$

$$\text{subject to} \quad |\mathbf{h}_c^H \mathbf{F}_L \mathbf{w}|^2 \geq q, \quad (20b)$$

$$\mathbf{w}_L^H \mathbf{F}_L^H \mathbf{F}_L \mathbf{w} = P_T, \quad (20c)$$

where  $\mathbf{w} \in \mathbb{C}^L$ . To address the nonconvex problem of (20), we consider a simple alternating minimization approach. For a fixed  $\mathbf{w}$ , the optimization over  $\mathbf{D}_T$  leads to a closed-form solution given by

$$[\mathbf{D}_T]_{nn} = e^{j\phi_n}, \quad \phi_n = \angle[\boldsymbol{\mu}^H \mathbf{A}_T^H \mathbf{F}_L \mathbf{w}]_n, \quad n = 1, \dots, N_g. \quad (21)$$

On the other hand, with a fixed  $\mathbf{D}_T$ , the optimization problem over  $\mathbf{w}$  becomes a quadratic program with two quadratic constraints, which is known to exhibit strong duality. As a result, this problem can be efficiently solved using Lagrange duality, leading to a closed-form solution (skipping the derivation details due to space limitations)

$$\mathbf{w} = (\Xi_0 + \lambda_1 \Xi_1 + \lambda_2 \Xi_2)^{-1} \tilde{\boldsymbol{\mu}}, \quad (22)$$

where  $\Xi_0 \triangleq \mathbf{F}_L^H \mathbf{A}_T \mathbf{A}_T^H \mathbf{F}_L$ ,  $\Xi_1 \triangleq \mathbf{F}_L^H \mathbf{h}_c \mathbf{h}_c^H \mathbf{F}_L$ ,  $\Xi_2 \triangleq \mathbf{F}_L^H \mathbf{F}_L$ ,  $\tilde{\boldsymbol{\mu}} \triangleq \mathbf{F}_L^H \mathbf{A}_T \mathbf{D}_T \boldsymbol{\mu}_T$ , and  $\lambda_{1/2}$  are Lagrange variables that can be determined using methods such as bisection. It alternates between (21) and (22) until convergence. It is noted that the same procedure can be applied to optimize the receive beamforming problem in (11) and the OMP subproblem in (17) with appropriate modifications.

### C. Remarks

The alternating minimization procedure is always guaranteed to converge to a local solution since the objective is non-increasing at every step. As a result, the overall performance largely depends on the two-way matching pursuit codeword selection in Stage I. Operationally, the algorithm first selects codewords more aligned with the direction of  $\mathbf{h}_c$  for the first  $\ell \leq L$  iterations until condition (14) is satisfied. Afterward, the remaining  $L - \ell$  codewords are chosen to enhance the sensing performance. Regarding the computational complexity, the algorithm is significantly more efficient than the brute force method, requiring only  $L$  iterations instead of  $\binom{K}{L}$ . Furthermore, the per-iteration complexity remains relatively low, as it is dominated by the minimization in (15) or in (17).

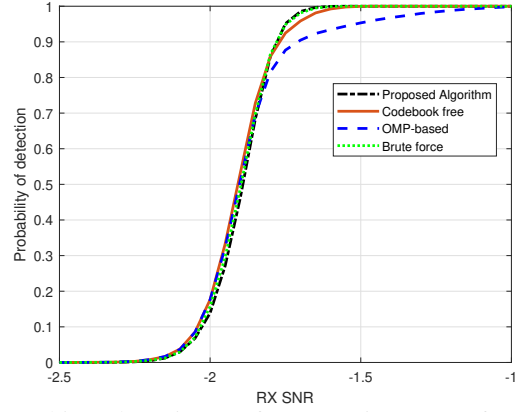


Fig. 4: Object detection performance in terms of probability of detection versus receiving (RX) SNR.

## IV. NUMERICAL EXAMPLES

We evaluated the performance of the proposed approach and the following baseline methods: I) the brute force method; II) a codebook-free solution which solves the transmit beamforming problem (10) without the codebook constraint (10b) and (10e); III) An OMP-based method to choose codewords based on the codebook-free solution [22]. To this end, we consider an AP equipped with  $N_T = 16$  transmit antennas and  $L = 4$  RF chains. The total transmit power is set to  $P_T = 10$  dBw. We use a codebook consisting of  $K = 24$  codewords on a uniform interval  $[-60^\circ, 60^\circ]$ . For communication, we adopt a line-of-sight channel where the user location is set to  $-50^\circ$  and the downlink communication SNR threshold is set to  $q = 10$  dB. The sensing interval of interest is set to  $[-15^\circ, 10^\circ]$ . The number of pre-determined grid values is  $N_g = 180$ .

First, we examine the transmit beampatterns generated by the proposed and considered baseline solutions in Fig. 3. It is noted that while the codewords selected by the proposed solution differ slightly from those chosen by the brute force method (differing on only one codeword out of  $L = 4$  in this instance), the proposed solution still provides a reasonably good approximation of the desired response over the sensing interval. Furthermore, we observe that the OMP baseline performs worse than the proposed solution, as evidenced by the presence of a notch over the sub-interval  $[5^\circ, 10^\circ]$ .

Next, we evaluate the performance of all considered methods for the task of detecting a target placed randomly in the sensing interval. We run Monte Carlo simulations with 1000 independent realizations, using the short training field (STF) from the DMG data frame for object detection. A standard matched filtering algorithm is employed for detection (see [20] for details). Fig. 4 shows the averaged probability of detection as a function of receiving SNRs for all considered methods. The results show that the proposed method matches the performance of the brute force method, while being computationally more efficient. Moreover, the proposed method slightly outperforms the codebook-free solution and delivers a much better performance than the OMP-based approach.

## V. CONCLUSION

This paper proposes a codebook-based beamforming design that aims to match a desired array response corresponding to targeted sensing areas while satisfying requirements on the downlink communication SNR to enable DTI Wi-Fi sensing. The proposed two-stage solution has low computational complexity and aligns with the upcoming 802.11bf WLAN Sensing.

## REFERENCES

- [1] R. Du *et al.*, “An overview on IEEE 802.11bf: WLAN sensing,” *IEEE Communications Surveys & Tutorials*, 2024.
- [2] P. Smulders, “Exploiting the 60 GHz band for local wireless multimedia access: prospects and future directions,” *IEEE Communications Magazine*, vol. 40, no. 1, pp. 140–147, 2002.
- [3] H. Xu, V. Kukshya, and T. Rappaport, “Spatial and temporal characteristics of 60-GHz indoor channels,” *IEEE Journal on Selected Areas in Communications*, vol. 20, no. 3, pp. 620–630, 2002.
- [4] T. Nitsche *et al.*, “IEEE 802.11ad: directional 60 GHz communication for multi-Gigabit-per-second Wi-Fi,” *IEEE Communications Magazine*, vol. 52, no. 12, pp. 132–141, 2014.
- [5] Y. Ghasempour *et al.*, “IEEE 802.11ay: Next-generation 60 GHz communication for 100 Gb/s Wi-Fi,” *IEEE Communications Magazine*, vol. 55, no. 12, pp. 186–192, 2017.
- [6] E. Grossi, M. Lops, L. Venturino, and A. Zappone, “Opportunistic radar in IEEE 802.11ad networks,” *IEEE Transactions on Signal Processing*, vol. 66, no. 9, pp. 2441–2454, 2018.
- [7] E. Grossi, M. Lops, and L. Venturino, “Adaptive detection and localization exploiting the IEEE 802.11ad standard,” *IEEE Transactions on Wireless Communications*, vol. 19, no. 7, pp. 4394–4407, 2020.
- [8] E. Grossi, M. Lops, A. M. Tulino, and L. Venturino, “Opportunistic sensing using mmwave communication signals: A subspace approach,” *IEEE Transactions on Wireless Communications*, vol. 20, no. 7, pp. 4420–4434, 2021.
- [9] J. Wang, J. Chuang, S. Berweger, C. Gentile, and N. Golmie, “Towards opportunistic radar sensing using millimeter-wave Wi-Fi,” *IEEE Internet of Things Journal*, pp. 1–1, 2023.
- [10] P. Wang and P. Boufounos, “Monostatic DMG passive sensing with hypothesis testing,” in *IEEE International Conference on Acoustics, Speech and Signal Processing (ICASSP)*, 2024, pp. 13 381–13 385.
- [11] M. Pajovic *et al.*, “Fingerprinting-based indoor localization with commercial MMWave WiFi—Part I: RSS and Beam Indices,” in *IEEE Global Communications Conference*, Dec. 2019.
- [12] P. Wang *et al.*, “Fingerprinting-based indoor localization with commercial mmwave WiFi—Part II: Spatial beam SNRs,” in *IEEE Global Communications Conference*, Dec 2019.
- [13] P. Wang, T. Koike-Akino, and P. V. Orlik, “Fingerprinting-based indoor localization with commercial mmwave WiFi: NLOS propagation,” in *IEEE Global Communications Conference*, December 2020.
- [14] T. Koike-Akino *et al.*, “Fingerprinting-based indoor localization with commercial mmwave WiFi: A deep learning approach,” *IEEE Access*, vol. 8, pp. 84 879–84 892, 2020.
- [15] J. Yu *et al.*, “Human pose and seat occupancy classification with commercial mmwave WiFi,” in *GLOBECOM Workshop on Integrated Sensing and Communication*, December 2020.
- [16] T. Koike-Akino, P. Wang, and Y. Wang, “Quantum transfer learning for Wi-Fi sensing,” in *IEEE International Conference on Communications*, May 2022, pp. 654–659.
- [17] C. J. Vaca-Rubio, P. Wang, T. Koike-Akino, Y. Wang, P. Boufounos, and P. Popovski, “Object trajectory estimation with continuous-time neural dynamic learning of millimeter-wave Wi-Fi,” *IEEE Journal of Selected Topics in Signal Processing*, vol. 18, no. 5, pp. 796–811, 2024.
- [18] Narengerile, D. Rui, M. Hu, Y. Xin, and A. Kasher, “DMG passive sensing based on A-BFT,” in *IEEE 802.11-22/423r0, Technical Contributions to 802.11bf WLAN Sensing Task Group*, 2024. [Online]. Available: <https://mentor.ieee.org/802.11/dcn/22/11-22-0423-00-00bf-dmg-passive-sensing-based-on-a-bft.pptx>
- [19] P. Kumari, N. Gonzalez-Prelcic, and R. W. Heath, “Investigating the IEEE 802.11ad standard for millimeter wave automotive radar,” in *IEEE VTC2015-Fall*, 2015, pp. 1–5.
- [20] P. Kumari, J. Choi, N. González-Prelcic, and R. W. Heath, “IEEE 802.11ad-based radar: An approach to joint vehicular communication-radar system,” *IEEE Transactions on Vehicular Technology*, vol. 67, no. 4, pp. 3012–3027, 2018.
- [21] G. Duggal, S. Vishwakarma, K. V. Mishra, and S. S. Ram, “Doppler-resilient 802.11ad-based ultrashort range automotive joint radar-communications system,” *IEEE Transactions on Aerospace and Electronic Systems*, vol. 56, no. 5, pp. 4035–4048, 2020.
- [22] C. Qi, W. Ci, J. Zhang, and X. You, “Hybrid beamforming for millimeter wave MIMO integrated sensing and communications,” *IEEE Communications Letters*, vol. 26, no. 5, pp. 1136–1140, 2022.